Journal of Photochemistry and Photobiology A: Chemistry 201 (2009) 183–190

Contents lists available at ScienceDirect

Journal of Photochemistry and Photobiology A: Chemistry

journal homepage: www.elsevier.com/locate/jphotochem

DNA-binding properties studies and spectra of a novel fluorescent Zn(II) complex with a new chromone derivative

Ju Wang, Zheng-Yin Yang*, Xu-Yang Yi, Bao-Dui Wang

College of Chemistry and Chemical Engineering and State Key Laboratory of Applied Organic Chemistry, Lanzhou University, Lanzhou 730000, PR China

ARTICLE INFO

Article history:
Received 12 June 2008
Received in revised form 23 October 2008
Accepted 24 October 2008
Available online 14 November 2008

Keywords:
Zn(II) complex
Chromone
Fluorescent properties
Calf thymus DNA
Intercalation mechanism

ABSTRACT

A new chromone derivative (6-ethoxy chromone-3-carbaldehyde benzoyl hydrazone) ligand (L) and its two transition metal complexes [Zn(II) complex and Ni(II) complex] have been prepared and characterized on the basis of elemental analysis, molar conductivity, mass spectra, UV–vis spectra and IR spectra. The Zn(II) complex exhibits light blue fluorescence under UV light, and the fluorescent properties of Zn(II) complex and the ligand in solid state and in different solutions (MeOH, DMF, THF and H_2O) were investigated. In addition, the interactions of the Zn(II) complex and the ligand with calf thymus DNA were investigated using UV–vis absorption, fluorescence, circular dichroic spectral methods and viscosity measurement. It was founded that both two compounds, especially the Zn(II) complex, strongly bind with calf thymus DNA, presumably via an intercalation mechanism.

© 2008 Elsevier B.V. All rights reserved.

1. Introduction

There has been considerable interest in the binding studies of small molecules to DNA. A more complete understanding of how to target DNA site would be valuable in the rational design of sequence-specific DNA-binding molecules of application in chemotherapy and highly sensitive DNA probe [1–3]. Given the structural flexibility and variable dimensionality, transition metal complexes play a key role in the development of new bound complex at a DNA site in recent years [4–10]. Basically, metal complexes interact with the double helix DNA in either a non-covalent or a covalent way. The former way includes three binding modes: intercalation, groove binding and external static electronic effects. Among these interactions, intercalation is one of the most important DNA-binding modes as it invariably leads to cellular degradation. Intercalative mode usually presents in compound of planar aromatic ring systems that occupy the space between two adjacent DNA base pairs. As both spectroscopic tags and functional models for the active centers, these complexes have been broadly used as foot-printing agents of both proteins and DNA.

Currently, due to their high antitumor activity and low toxicity, some natural products are being paid attention. Chromones are ubiquitous in nature especially in plants. These natural products are potentially antibacterial, anticancer, antioxidant, anti-inflammatory, and antiallergenic agents since they stimulate or inhibit a wide variety of enzyme systems as pharmacological agents [11,12]. Our previous work showed that 6-hydroxy chromone-3-carbaldehyde hydrazones and their Ln(III) complexes can bind to CT-DNA via intercalative mode, and their complexes have diverse spectral properties, certain antitumor and antioxidative activities [13–17]. It is well known that the different substituting group and conformation can affect the binding mode of compound with DNA.

Based on these evidences, in this study, we synthesized a novel chromone hydrazone ligand (6-ethoxy chromone-3-carbaldehyde benzoyl hydrazone) and its two transition metal complexes. We explored the binding mode of the ligand and Zn(II) complex with CT-DNA using spectroscopic and hydrodynamic methods. The fluorescent properties of Zn(II) complex in solid state and different solvents were also studied. The results should be extremely useful for understanding the mode of the complex with DNA as well as laying a foundation for the rational design of novel, powerful agents for probing and targeting nucleic acids. This study will be very helpful to examine the DNA conformation and structure.

2. Experimental

2.1. Materials

All chemicals used were of analytical grade and purchased from commercial vendors.

Calf thymus DNA (CT-DNA) was obtained from Sigma. UV–vis spectrometer was employed to check DNA purity 1.8–1.9:1 and

* Corresponding author. Tel.: +86 931 8913515; fax: +86 931 8912582.
E-mail address: yangzy@lzu.edu.cn (Z.-Y. Yang).

1010-6030/$ – see front matter © 2008 Elsevier B.V. All rights reserved.
doi:10.1016/j.jphotochem.2008.10.022

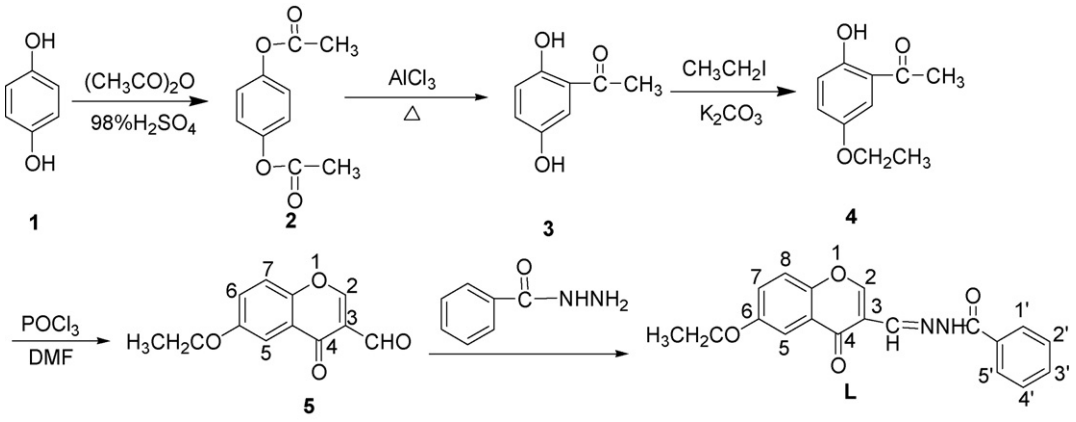

Fig. 1. Scheme of the synthesis of the ligand (L).

concentration ($\varepsilon = 6600\,M^{-1}\,cm^{-1}$ at 260 nm) [18–19]. All the experiments involving interaction of the compounds with DNA were carried out in doubly distilled water buffer containing 5 mM Tris [Tris (hydroxymethyl)-aminomethane] and 50 mM NaCl, and adjusted to pH 7.2 with hydrochloric acid.

2.2. Physical measurements

The metal ions were determined by EDTA (ethylene diamine tetraacetic acid) titration using xylenol orange as an indicator. Carbon, nitrogen and hydrogen analyses were determined using a Vario EL analyzer. Molar conductivity measurements were carried out with a DDS-11C type conductivity bridge using 1.0×10^{-3} mol/l solutions in methanol at 25 °C. IR spectra were recorded on a Thermo Mattson FT-IR instrument using KBr discs in the 4000–400 cm^{-1} region. The UV–vis spectra were recorded on a PerkinElmer Lambda-35 UV–vis (Ultraviolet and Visible) spectrophotometer. ^1H NMR spectrum was measured on a Bruker DRX-200 200-MHz spectrometer in solution with TMS as internal standard. Electrospray ionization (ESI) mass spectrometry was recorded on APEX II FT-ICR MS using methanol as mobile phase. Circular dichroism spectra of DNA were obtained by using JASCO J-810 spectropolarimeter operated at room temperature. Melting points were determined on a Beijing XT4-100X microscopic melting point apparatus. Fluorescence spectra and fluorescence quantum yields were obtained on a Shimadzu RF-5301 spectrophotometer at room temperature, and the latter used a quinine sulfate in 1 mol/l H_2SO_4 ($\Phi_f = 0.546$) [20] as a standard.

2.3. Preparation of ligand and complexes

2.3.1. Synthesis of the ligand (L)

The organic compounds **1**–**3** (Fig. 1) were prepared according to literature [21].

The organic compound **4** (Fig. 1): A mixture of **3** (7.60 g, 50 mmol), 60 mmol of the proper alkyl halide (10.46 g, 75.8 mmol), of anhyd. K_2CO_3 and acetone (220 ml) was heated at reflux for 2–3 d, with stirring. The mixture was filtered off, washed with acetone and the brown filtrate was concentrated to a solid. The solid was chromatographed on a silica gel column, eluting with acetate-petroleum ether (1:20) to give, after removal of solvents from the eluate collected, the nearly pure yellow crystals of compound **4**.

Yield: 70%. m.p.: 50 °C ([22] m.p.: 52 °C). Anal. Calcd for $C_{10}H_{12}O_{43}$: C, 66.65; H, 6.71. Found: C, 66.60; H, 6.80. ^1H NMR ($CDCl_3$): δ 11.84 (1H, s, OH), 7.64–7.33 (3H, m, PhH), 4.01 (2H, q, CH_2), 2.62 (3H, s, $COCH_3$), 1.42 (3H, t, CH_3). IR (KBr) cm^{-1}: ν (C=O) 1643, 1620, 1587, 1484.

The organic compound **5** (Fig. 1): compound **4** (3.60 g, 20 mmol) was dissolved in DMF (40 ml), then $POCl_3$ (20 ml) was added to the above solution at 0 °C. The mixture solution was stirred at room temperature overnight. The solution was allowed to stir at 100 °C for 1 h. The mixture was added to ice water yielding a precipitate, which was filtered off, washed with water and dried. Then the solid was chromatographed on a silica gel column, eluting with ethyl acetate-petroleum ether (1:30) to give, after removal of solvents from the eluate collected, the nearly pure yellow compound **5**.

Yield: 60%. m.p.: 134–135 °C. Anal. Calcd for $C_{12}H_{10}O_4$: C, 66.05; H, 4.62. Found: C, 66.60; H, 4.70. ^1H NMR ($CDCl_3$): δ 10.41 (1H, s, CHO), 8.53 (1H, s, 2-H), 7.64–7.33 (3H, m, 5, 7, 8-H), 4.16 (2H, q, CH_2), 1.47 (3H, t, CH_3). IR (KBr) cm^{-1}: ν (C=O) 1700, ν (CHO) 1640.

The ligand (L) (Fig. 1) was synthesized as follows. An ethanol solution containing benzoyl hydrazone (1.36 g, 10 mmol) was added dropwise to another ethanol solution containing **5** (2.31 g, 10 mmol). The mixture was stirred for 1 h at room temperature yielding a precipitate, which was filtered off, washed with ethanol and dried in a vacuum. The solid was recrystallized from ethanol to yield a yellow solid and then dried.

Yield: 80%. m.p.: 159 °C. Anal. Calcd for $C_{19}H_{16}N_2O_4$: C, 67.85; H, 4.79, N, 8.33. Found: C, 67.80; H, 4.85; N, 8.27. HRMS [CH_3OH, m/e]: 337.1194 (calcd for $C_{19}H_{17}N_2O_4$: 337.1188). ^1H NMR (DMSO): δ 11.93 (1H, s, NH), 8.63 (1H, s, 2-H), 8.81 (1H, s, CH=N), 7.94–7.41 (8H, m, 5, 7, 8-H, PhH (2′,3′,4′)), 4.16 (2H, q, CH_2), 1.37 (3H, t, CH_3). HRMS [CH_3OH, m/e]: 337.1194 (calcd for $C_{19}H_{17}N_2O_4$: 337.1188). IR (KBr) cm^{-1}: ν $(C{=}O)_{(hydrazonic)}$ 1650, ν $(C{=}O)_{(carbonyl)}$ 1626, ν (C=N) 1602. UV λ_{max} (MeOH) nm (ε): 213 (27,730), 291 (15,590), 321 (17,370), 410 (12,780).

2.3.2. Synthesis of the complexes

The ligand (L) (0.17 g, 0.5 mmol) was dissolved in acetone (10 ml) when refluxed on an oil-bath at 70 °C with stirring. To this solution was added dropwise a solution of $Zn(NO_3)_2{\cdot}6H_2O$ (0.15 g, 0.5 mmol) in acetone (5 ml). Immediately, a large amount of white precipitate appeared. The precipitate was separated from the solution by centrifuge, purified by washing several times with acetone and dried for 24 h in a vacuum. The Ni(II) complex was also synthesized as the above method.

Zn(II) complex $[ZnLNO_3]NO_3$: color: white, yield: 80%. Anal. Calcd for $C_{19}H_{16}N_4O_{10}Zn$: C, 43.41; H, 3.07; N, 10.66; Zn, 12.44. Found: C, 43.14; H, 2.91; N, 10.44; Zn, 12.70. HRMS [CH_3OH, m/e]: 462.0243 (calcd for $C_{19}H_{16}N_3O_7Zn$: 462.0280), 399.0276 (calcd for $C_{19}H_{15}N_2O_4Zn$ 399.0323). IR (KBr) cm^{-1}: ν $(C{=}O)_{(hydrazonic)}$ 1640, ν $(C{=}O)_{(carbonyl)}$ 1612, ν (C=N) 1579, ν_1 (NO_3) 1487, ν_0 (NO_3) 1384, ν_4 (NO_3) 1321, ν (M–O) 577, ν (M–N) 427. UV λ_{max} (MeOH) nm (ε): 202 (57,270), 329 (14,940), 410 (20,410). Λm ($S\,cm^2\,mol^{-1}$): 140.7.

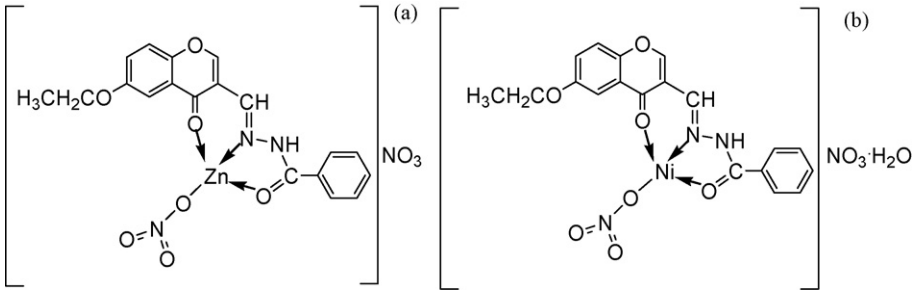

Fig. 2. Proposed structure of the complexes. (a) The Zn(II) complex and (b) the Ni(II) complex.

Ni(II) complex $[NiLNO_3]NO_3 \cdot H_2O$: color: blue, yield: 80%. Anal. Calcd for $C_{19}H_{18}N_4O_{11}Ni$: C, 42.49; H, 3.38; N, 10.43; Ni, 10.93. Found: C, 42.75; H, 3.51; N, 10.23; Ni, 11.20. IR (KBr) cm^{-1}: ν $(C{=}O)_{(hydrazonic)}$ 1642, ν $(C{=}O)_{(carbonyl)}$ 1612, ν (C=N) 1577, ν_1 (NO_3) 1471, ν_0 (NO_3) 1384, ν_4 (NO_3) 1327, ν (M–O) 579, ν (M–N) 429. UV λ_{max} (MeOH) nm (ε): 203 (83,910), 326 (33,340), 412 (13,260). Λm ($S\,cm^2\,mol^{-1}$): 98.2.

2.4. DNA-binding affinity study methods

2.4.1. UV absorption titration

Absorption titration experiment was performed by maintaining the ligand and metal complex concentration constant (10 μM) and gradually increasing the concentration of nucleic acid. The compounds were dissolved in a mixed solvent of 1% CH_3OH and 99% Tris–HCl buffer (5 mM Tris–HCl, 50 mM NaCl, pH 7.2). The reference solution was the corresponding Tris–HCl buffer solution. While measuring the absorption spectra, equal amount of CT-DNA was added to both compound solution and the reference solution to eliminate the absorbance of CT-DNA itself. Each sample solution was scanned in the range 200–500 nm.

2.4.2. Fluorescence titration

To compare quantitatively the affinity of the compound bound to CT-DNA, the intrinsic binding constants K_b of the two compounds binding to CT-DNA were obtained by the fluorescence titration method. The samples were excited at their corresponding isosbestic points. All the measurements were made at room temperature with 5 nm for both entrance and exit slit. Fixed amounts of the compound (10 μM) were titrated with increasing amounts of CT-DNA. An excitation wavelength of 330 nm was used, and total fluorescence emission intensity was monitored at 428 nm for the ligand and 424 nm for Zn(II) complex.

2.4.3. Circular dichroism (CD)

CD spectra were recorded on a J-810 JASCO spectropolarimeter at room temperature. A rectangular quartz cell of 1 cm path length was used to obtain spectra from 320 to 220 nm with a scanning speed 100 nm/min. The optical chamber of the CD spectrometer was deoxygenated with dry nitrogen before use and kept in a nitrogen atmosphere during experiments. Scans were accumulated and automatically averaged. A CD spectrum was generated which represented the average of three scans from which the buffer background had been subtracted. Titrations of CT-DNA with the compounds were performed with a fixed CT-DNA concentration (100 μM) and increasing concentrations of compounds (0, 50 μM).

2.4.4. Viscosity measurements

Viscosity experiments were carried out on an Ubbelohde viscometer, immersed in a thermostatic water bath maintained at $25.0 \pm 0.1\,^{\circ}C$. DNA concentration was kept constant (5 μM) and gradually increased the concentration of tested compound (0.5–3 μM). Flow time was measured with a stopwatch. Each sample was measured three times and an average flow time was calculated.

3. Results and discussion

3.1. Characterization of compounds

3.1.1. Properties of the compounds and structure of the complexes

The ligand is soluble in acetone and acetonitrile, while the two complexes are insoluble in both of them. The three compounds are soluble in DMF (N, N-dimethylformamide), DMSO (dimethyl sulfoxide), THF (tetrahydrofuran), methanol, slightly soluble in ethanol, insoluble in water and diethyl ether. All of them are air stable for at least 6 months. The elemental analyses show that the formulas of the complexes conform to $ML(NO_3)_2 \cdot nH_2O$ (M = Zn, n = 0 and M = Ni, n = 1). The molar conductivity of the complexes in methanol are 140.7 and 98.2 $S\,cm^2\,mol^{-1}$, which are in the range expected for 1:1 electrolytes [23]. Since the crystal structure of the complexes have not been obtained yet, we characterized the complexes and determined their possible structure by elemental analyses, molar conductivities, MS spectra, IR data and UV–vis measurements, the likely structure of the complexes is shown in Fig. 2.

3.1.2. IR spectra

The IR of the ligand and its complexes are presented in Section 2. On the basis of the similar IR spectra of the Zn(II) and Ni(II) complexes, it may be assumed that they have similar coordination structures. From the major IR data, the ν $(C{=}O)_{(hydrazonic)}$ and ν $(C{=}O)_{(carbonyl)}$ vibrations of the free ligand are at 1650 and 1626 cm^{-1}, respectively; for the two complexes these peaks shift to about 1640 and 1612 cm^{-1} or so, $\Delta\nu_{(ligand\text{-}complex)}$ is equal to 10 and 14 cm^{-1}. The new band at 577 and 579 cm^{-1} for the two complexes are assigned to ν (M–O) [15]. These shifts and the new band demonstrate that the oxygen of carbonyl has formed a coordinative bond with the metal ion. The band at 1602 cm^{-1} for the free ligand is assigned to the ν (C=N) stretch, which shifts to 1579 and 1577 cm^{-1} for its Zn(II) and Ni(II) complexes, respectively. Weak bands at 427 and 429 cm^{-1} for the two complexes are assigned to ν (M–N) [13,17]. These shifts and the new bands further confirm that the nitrogen of the amino-group bonds to the metal ion. Additionally, the two intense absorption bands in the spectra associated with the asymmetric stretching appear in the range of 1321 cm^{-1} (ν_4) and 1487 cm^{-1} (ν_1) or so, clearly establishing that there are some coordinated nitrates groups (C_{2v}) in the complexes [24]. The differences between the two bands lie in 166 and 144 cm^{-1}, suggesting that the coordinated nitrate groups in the complexes are monodentate [25]. For the complexes, bands at 1384 cm^{-1} in the spectra of complexes indicate that free nitrate groups (D_{3h}) exist [26]. The conclusion is also supported by the results of the conductivity experiments.

3.1.3. UV–vis spectra

The study of the electronic spectra in the ultraviolet and visible ranges for the ligand and its complexes were carried out in methanol solution. The electronic spectra of ligand had a strong band at λ_{max} = 213 nm, two medium bands at λ_{max} = 291 and 321 nm and a weak band at λ_{max} = 410 nm. In the complexes, the band at λ_{max} = 295 nm disappeared. The one band at λ_{max} = 213 nm was blue-shifted to λ_{max} = 202 nm or so. The bands at λ_{max} = 410 nm or so are stronger than that in the ligand. The band of Zn(II) and Ni(II) at λ_{max} = 321 nm was red-shifted to λ_{max} = 329 nm or so. These indicate that the complexes are formed.

3.1.4. MS spectra

Electrospray ionization (ESI) mass spectrum of the Zn(II) complex is shown in Fig. 3 and the proposed degradation of the Zn(II) complex is demonstrated in Fig. 4. The mass spectrum of Zn(II) complex shows peaks at m/e of 462.0243 (calcd: 462.0280), 399.0276 (calcd: 399.0323), which can be assigned to the ion pair $[ZnLNO_3]^+$, $[ZnL\text{-}H]^+$, respectively. These are in accordance with the other means of characterization.

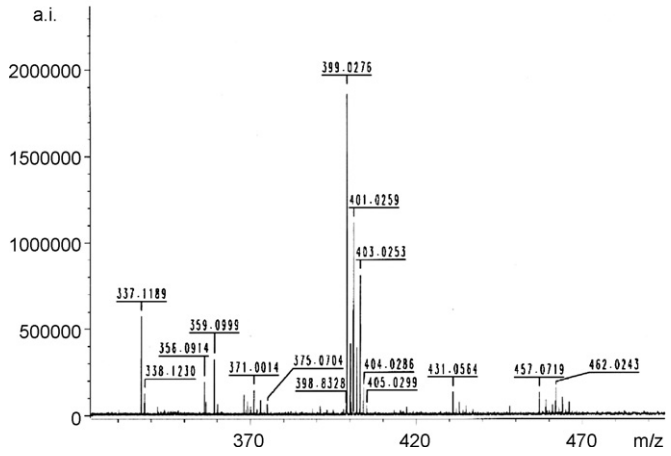

Fig. 3. Electrospray ionization (ESI) mass spectrum of the Zn(II) complex.

3.1.5. Fluorescence spectra

The Zn(II) complex exhibits light blue fluorescence and the emission is readily observed with naked eye under UV light, which is shown in Fig. 5(a). However, in the solid state the fluorescence intensity of the Ni(II) complex is much too weak, which is not discussed in this work. Fluorescent spectra of the ligand and the Zn(II) complex in solid state are shown in Fig. 5(b). The free ligand has very weak emission (at 482 nm) in the visible region. In contrast to the free ligand, Zn(II) complex has a strong blue luminescence with an emission maximum at 433 nm in the solid state. The fluorescence intensity at 433 nm is 16.5 times of that of the ligand at 482 nm. Because $Zn(NO_3)_2$ has no fluorescence, the observed blue fluorescence is attributed to the coordinated ligand. The Zn(II) complex is the first example of blue-fluorescent complex with chromone hydrazone ligands. We have previously reported red-fluorescent Sm(III) and Eu(III) compounds with 6-hydroxy chromone hydrazone ligands [13–16].

Compared with the emission band (at 482 nm) of ligand, the emission band of complex is blue-shift to 433 nm, under the same excitation. This anomaly can be explained by the fact that excited state resulting from the Zn(II) complex is typically ligand-centered

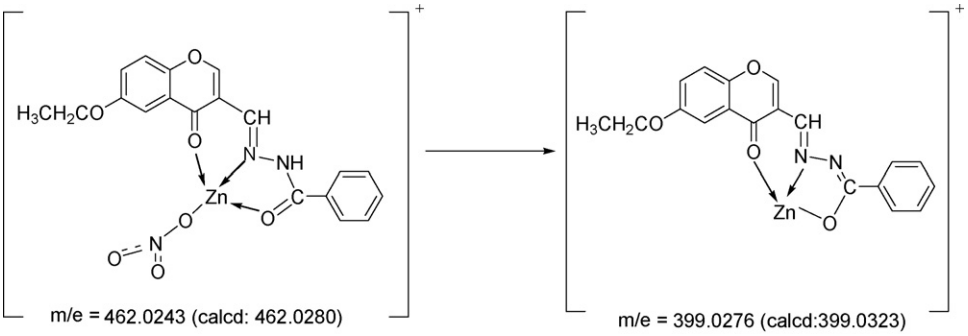

Fig. 4. Proposed degradation of the Zn(II) complex.

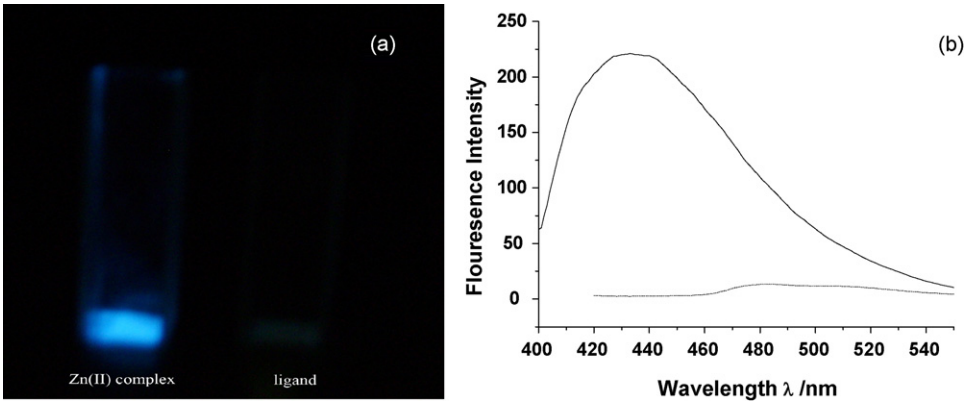

Fig. 5. (a) The Zn(II) complex (left) and the ligand (right) are excited with the UV light (solid sample in quartz cuvette). (b) Solid-state emission spectra of the ligand and the Zn(II) complex—solid line: Zn(II) complex (excited wavelength: 384 nm); dashed line: ligand (excited wavelength: 408 nm). All the excitation and emission slit widths were 3 nm.

Table 1
Fluorescence spectra data and fluorescence quantum yield Φ_f of the Zn(II) complex and the ligand in different solutions (concentration = 2.5 μM) at room temperature. All the excitation and emission slit widths were 3 nm.

Compound	Solvent	Excitation λ (nm)	Emission λ (nm)	Emission intensity	Φ_f
Zn(II) complex	THF	307	406	10.933	0.0351
	Methanol	303	443	37.479	0.2611
	DMF	308	412	118.046	0.1924
	H_2O (0.1% methanol)	304	430	4.466	0.0484
Ligand	THF	305	397	7.745	0.0293
	Methanol	303	399	5.432	0.0313
	DMF	308	412	116.886	0.1724
	H_2O (0.1% methanol)	307	429	4.288	0.0218

(LC) in nature, owing to the inability of the d^{10} metal center to participate in low-energy charge-transfer or metal-centered transitions [27].

Solution emission and excitation spectra of the two compounds were also measured (Table 1). The blue-shift of the compounds energy from solution to solid is likely to be caused by the intermolecular. While the fluorescence intensity of Zn(II) complex, relative to that of the free ligand, is dramatically enhanced, which is clearly caused by the formation of coordination bonds between the ligand and the zinc ion. In addition, the solution fluorescent spectra of the ligand and Zn(II) complex are highly solvent-dependent.

The formation of complex appears to enhance the emission efficiency of the ligand. Relative to that of quinine sulfate, the fluorescence quantum yields for Zn(II) complex in THF, methanol DMF and H_2O (0.1% methanol) solutions were determined to be 0.0351, 0.2611, 0.1924 and 0.0484, respectively, significantly higher than that of the ligand 0.0293, 0.0313, 0.1724 and 0.0218 under the same condition. Furthermore, compared with that of quinine sulfate (absolute fluorescence quantum yield $\Phi_f = 0.546$), the Zn(II) complex exhibits a certain high fluorescence quantum yields, indicating that Zn(II) complex in methanol has the potential to be a blue emitter in electroluminescent (EL) devices.

3.2. DNA-binding mode and affinity

3.2.1. UV–vis absorption titration

The binding of intercalative drugs to DNA has also been characterized classically through absorption titrations, following the hypochromism and red shift associated with binding of the colored complex to the helix [28]. These spectral characteristics are attributable to a mode of binding that involves an interaction between an aromatic chromophore and the base pairs of DNA. The magnitudes of the red shift and the degree of hypochromism are furthermore commonly found to correlate with the strength of the intercalative interaction [29]. Fig. 6(a) and (b) shows absorption titration for the ligand and Zn(II) complex as a function of DNA addition. The electronic spectrum of ligand has a strong band at 221 nm, a medium band at 323 nm. The ligand at 221 and 323 nm exhibit hypochromism of about 20.84 and 28.41%, and red shift of about 3 and 1 nm. While in the spectra of the Zn(II) complex, the intense absorption bands with maxima of 202, 291 and 315 nm are observed, which is different from the ligand. In the presence of CT-DNA, the absorption bands of Zn(II) complex at 291, 315 nm exhibit hypochromism of about 58.13%, 51.69%, the red shift of about 12 and 6 nm, respectively. However, the band at 202 nm only exhibits hypochromism 21.08% and no evident red shift. It is noteworthy that the hypochromicity of the complex is greater than that of the present ligand.

Base on the spectral characteristics, we presume that there are some interactions between the compounds and DNA.

3.2.2. Fluorescence titration

The ligand and its Zn(II) complex can emit weak luminescence in Tris-buffer with a max emission wavelength of about 433 nm. Figs. 7 and 8 display a well-behaved titration of the ligand and Zn(II) complex with CT-DNA. Increases in emission are apparent with DNA addition. The results of the emission titrations suggest that the two compounds get into a hydrophobic environment inside the DNA and avoid the quenching effect of solvent water molecules. The binding of Zn(II) complex and ligand to DNA leading to a marked increased in emission intensity also agrees with those observed for other intercalators [15–18]. Moreover, the similarity in spectroscopic perturbations indicates that two compound bind to DNA in a similar fashion.

To compare quantitatively the affinity of the compound bound to DNA, the intrinsic binding constants K_b of the two compounds

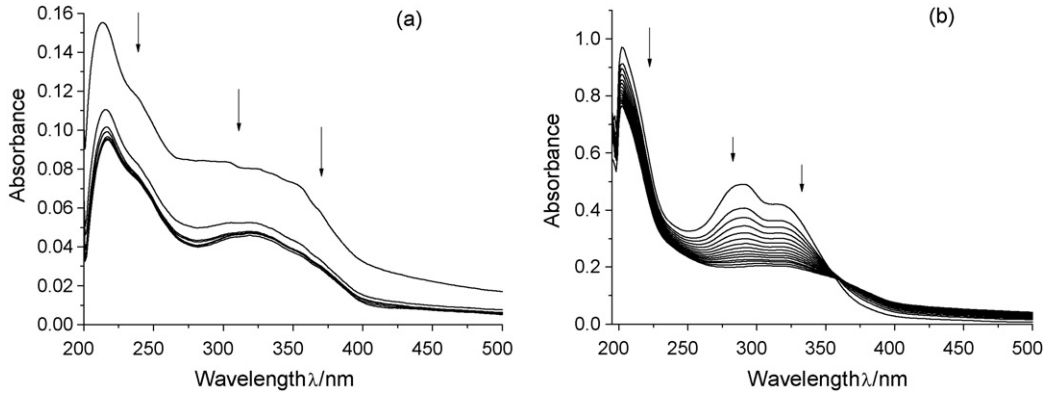

Fig. 6. (a) Electronic spectra of ligand complex (10 μM) in the presence of increasing amounts of CT-DNA, [DNA] = 0–14 μM. Arrow shows the absorbance changes upon increasing DNA concentration. (b) Electronic spectra of Zn(II) complex (10 μM) in the presence of increasing amounts of CT-DNA. [DNA] = 0–28 μM. Arrow shows the absorbance changes upon increasing DNA.

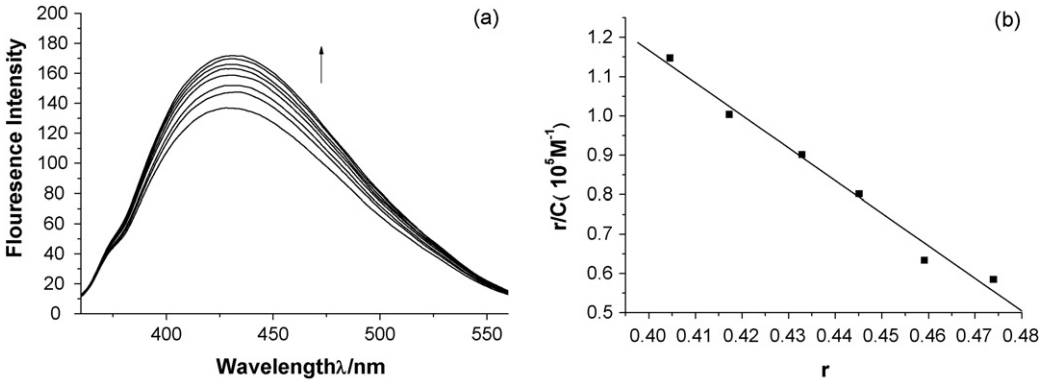

Fig. 7. (a) The emission enhancement spectra of ligand (10 μM) in the presence of 0–14 μM CT-DNA. Arrow shows the emission intensities upon increasing DNA concentration. (b) Scatchard plot of the fluorescence titration on data of ligand, intrinsic binding constant, $K_b = (8.27 \pm 0.52) \times 10^5\ M^{-1}$.

based upon these fluorescence titrations may be made with according to the Scatchard equation [30] and equations in [18].

$$\frac{r}{C_f} = K_b(n - r) \quad (1)$$

$$C_b = C_t \left[\frac{(F - F^0)}{(F^{max} - F^0)} \right]$$

$$C_f = C_t - C_b \quad (2)$$

$$r = \frac{C_b}{C_{DNA}}$$

where C_f is the free compound concentration, n is the number of binding sites, r is the binding ratio and K_b is the binding constant. C_t is the total compound concentration; F is the observed fluorescence emission intensity at a given DNA concentration; F^0 is the intensity in the absence of DNA, and F^{max} is the fluorescence of the totally bound compound. Binding data were cast into the form of a Scatchard plot [30] of r/C_f versus r. The binding constants K_b are $(8.27 \pm 0.52) \times 10^5\ M^{-1}$, $(1.09 \pm 0.01) \times 10^6\ M^{-1}$ for the ligand and Zn(II) complex, respectively. The data show that the interaction of the Zn(II) complex with DNA is stronger than that of the ligand, which is consistent with the above UV–vis absorption titration.

When compared the intrinsic binding constant (K_b) of two compounds with those of reported DNA-intercalative compounds (the K_b values are 10^5–$10^6\ M^{-1}$) [13,15–17,31,32], we may deduce that two compounds bind to DNA by intercalation. In the previous work from our laboratory, we have presented a detailed investigation of the interactions of chromone Schiff-Base and their Ln(III) complexes with DNA (CT-DNA) [13,15–17]. The binding constants (K_b) increase in the series 6-hydroxy chromone-3-carbaldehyde 2-hydroxy benzoyl hydrazone ($1.33 \times 10^6\ M^{-1}$) <6-hydroxy chromone-3-carbaldehyde benzoyl hydrazone ($2.41 \times 10^6\ M^{-1}$) <ethylenediaminebi (6-hydroxy chromone-3-carbaldehyde) ($4.88 \times 10^6\ M^{-1}$). In this paper, the binding constant (K_b) for the ligand (L) 6-ethoxy chromone-3-carbaldehyde benzoyl hydrazone chromone is $(8.27 \pm 0.52) \times 10^5$. After corrections for the affinities of different ligand, it appears from these data that the substituting group of ligand can affect the DNA-binding affinity. This variation likely reflects the differing ability of these ligands to stack and overlap well with the base pairs. In this paper, the hydroxyl group of 6-hydroxy chromone-3-carbaldehyde benzoyl hydrazone was substituted by ethoxy. Compared with the hydroxy, the ethoxy is a large group in space, which is not favorable to corresponding ligand intercalation with DNA. Hence, it is reasonable to understand why the ligand in this paper show a low magnitude of the red shift in UV–vis absorption as well as lower intrinsic binding constants compared with our previously reported ligand ($K_b = (2.41 \pm 0.46) \times 10^6\ M^{-1}$) [17]. Considering the Zn(II) complex, probably, chelating effect (metal ion to free ligand) can enhance the planar functionality of metal complex, so the complexes can insert and stack between the base pairs of double helical DNA more easily than the free ligand [33].

3.2.3. Circular dichroism (CD) studies

Circular dichroic spectral technique is useful in diagnosing changes in DNA morphology during drug–DNA interactions, as the band due to base stacking (275 nm) and that due to right-handed helicity (248 nm) are quite sensitive to the mode of DNA interactions with small molecules [34]. The changes in CD signals of DNA

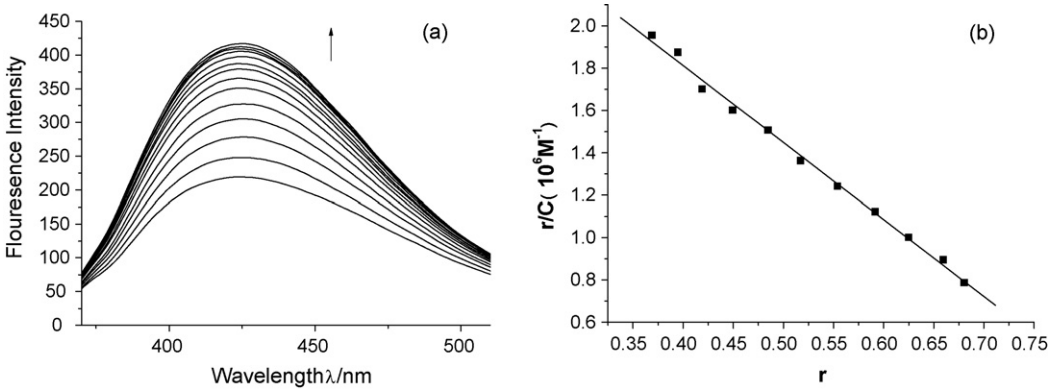

Fig. 8. (a) The emission enhancement spectra of Zn(II) complex (10 μM) in the presence of 0–26 μM CT-DNA. Arrow shows the emission intensities upon increasing DNA concentration. (b) Scatchard plot of the fluorescence titration data of Zn(II) complex, intrinsic binding constant, $K_b = (1.09 \pm 0.01) \times 10^6\ M^{-1}$.

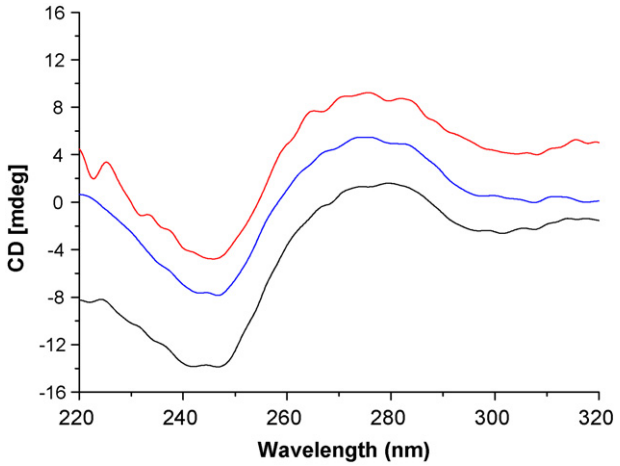

Fig. 9. CD spectrum of CT-DNA in the absence (Black line) and presence of the ligand (blue line) and the Zn(II) complex (red line), $r = 0.5$ (r = molar ratio [compound]/[CT-DNA]). (For interpretation of the references to color in this figure legend, the reader is referred to the web version of the article.)

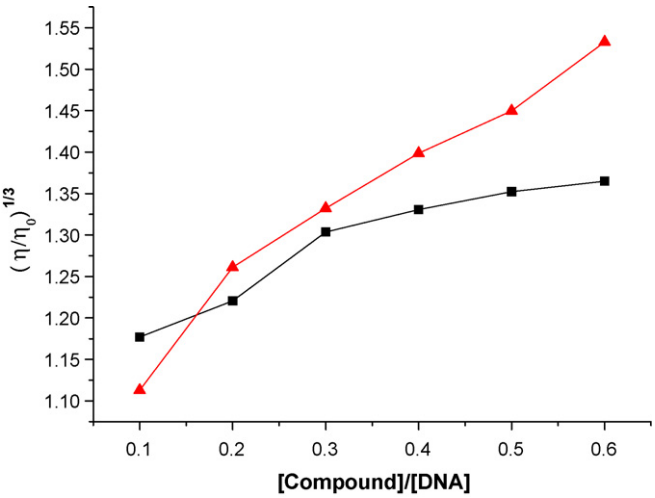

Fig. 10. Effect of increasing amounts of Zn(II) complex (▲) and ligand (■) on the relative viscosity of CT-DNA at 25 ± 0.1 °C [DNA] = 5 μM.

observed on interaction with drugs may often be assigned to the corresponding changes in DNA structure [35]. Thus simple groove binding and electrostatic interaction of small molecules show less or no perturbation on the base stacking and helicity bands, while intercalation enhances the intensities of both the bands stabilizing and the right-handed B conformation of CT-DNA as observed for the classical intercalator methylene blue [36]. The circular dichroic spectrum of CT DNA (Fig. 9) exhibits a positive band at 279 nm due to base stacking and a negative band at 246 nm due to helicity of B DNA [34]. Incubation of the DNA with the present compounds induced changes in the CD spectrum. When the present series of compounds are incubated with CT-DNA at r (r = molar ratio [compound/[CT-DNA]) value of 0.5, the CD spectrum of DNA undergoes changes in both the positive and negative bands. The ligand and the Zn(II) complex show intensity increase and decrease in the positive and negative bands, with the latter being affected slightly more than the other. However, there were not evident shifts in the band positions. A similar observation made for $[Ru(NH_3)_4(pip)]^{2+}$, $[Ru(NH_3)_4(hpip)]^{2+}$ and $[Ru(NH_3)_4(dip)]^{2+}$ bound to CT-DNA have been ascribed to a conformational conversion from a more B-like to a more A-like structure within the DNA molecule [37]. This reveals the effect of strong intercalation of the compounds on base stacking and decreased right-handedness of CT DNA as well [34].

Besides, the intensity increase observed for the complex is the higher than the ligand, which also indicates that binding strength of complex is much stronger than that of free ligand.

3.2.4. Viscosity measurements

Photophysical studies have proven quite useful in determining binding modes of metal complexes to DNA [38], but not sufficient clues to support a binding mode. The modes of binding of the complexes were further investigated by hydrodynamic measurements such as viscosity. A classical intercalation model demands that the DNA helix lengthens as base pairs are separated to accommodate the bound ligand, leading to the increase of DNA viscosity. In contrast, a partial, non-classical intercalation of ligand could bend (or kink) the DNA helix reduce its effective length and, concomitantly, its viscosity [18,39]. As a means for further clarifying the binding of these compounds with DNA, viscosity studies were carried out. Data are presented as $(\eta/\eta_0)^{1/3}$ versus R, where R = [Compound]/[DNA]; η and η_0 are the relative viscosities of DNA in the presence and absence of compound, respectively. The relative viscosity values were calculated from the flow time of DNA-containing solution t and the flow time of buffer alone t_0, using the following Eq. (3) [40]:

$$\eta = t - t_0 \tag{3}$$

The results of the viscosity measurements are shown in Fig. 10. On increasing the amount of ligand and Zn(II) complex, the relative viscosity of DNA increase steadily, The results suggest the two compounds may bind to DNA by intercalation.

4. Conclusion

In summary, a new chromone derivative (6-ethoxy chromone-3-carbaldehyde benzoyl hydrazone), and its two transition metal complexes [Zn(II) complex and Ni(II) complex] have been prepared and characterized. The Zn(II) complex is blue-fluorescent in the solid state, and the emission of the Zn(II) complex is highly solvent-dependent. Furthermore, the DNA-binding properties of the ligand and its Zn(II) complex were investigated by spectra titration and viscosity measurements. The two compounds all appear to intercalate into DNA. The conclusion is based upon the effects of hypochromism, the increases in emission intensities, changes in both the positive and negative bands of B-DNA and the increased degree of viscosity. Chelating effect (metal ion to free ligand) can enhance the planar functionality of metal complex, so the Zn(II) complex can insert and stack between the base pairs of double helical DNA more easily than the free ligand. This work also find that substituting group with chromone hydrazone ligands can affect the DNA-binding affinity. This work will be helpful to the understanding of the mechanism of compounds with nucleic acids, and useful in the development of potential probes of DNA structure and conformation.

Acknowledgements

This work is supported by the National Natural Science Foundation of China (20475023) and Gansu NSF (3ZS041-A25-016).

References

[1] B.N. Trawick, A.T. Daniher, J.K. Bashkin, Chem. Rev. 98 (1998) 939–960.
[2] K.E. Erkkila, D.T. Odom, J.K. Barton, Chem. Rev. 99 (1999) 2777–2795.
[3] D.S. Sigman, A. Mazumder, D.M. Perrin, Chem. Rev. 93 (1993) 2295–2316.
[4] P.J. Dandliker, R.E. Holmlin, J.K. Barton, Science 275 (1997) 1465–1468.

[5] D.B. Hall, R.E. Holmlin, J.K. Barton, Nature 382 (1996) 731–735.
[6] A.E. Friedman, J.C. Chambron, J.P. Sauvage, N.J. Turro, J.K. Barton, J. Am. Chem. Soc. 112 (1990) 4960–4962.
[7] P. Lincoln, A. Broo, B. Norden, J. Am. Chem. Soc. 118 (1996) 2644–2653.
[8] R.M. Hartshorn, J.K. Barton, J. Am. Chem. Soc. 114 (1992) 5919–5925.
[9] A. Sitlani, E.C. Long, A.M. Pyle, J.K. Barton, J. Am. Chem. Soc. 114 (1992) 2303–2312.
[10] L.N. Ji, X.H. Zou, J.G. Liu, Coord. Chem. Rev. 216/217 (2001) 513–536.
[11] P.F. Wiley, J. Am. Chem. Soc. 74 (1952) 4326–4328.
[12] J. Marmur, J. Mol. Biol. 3 (1961) 208–218.
[13] B.D. Wang, Z.Y. Yang, T.R. Li, Bioorg. Med. Chem. 14 (2006) 6012–6021.
[14] B.D. Wang, Z.Y. Yang, D.W. Zhang, Y. Wang, Spectrochim. Acta, Part A 63 (2006) 213–219.
[15] B.D. Wang, Z.Y. Yang, D.D. Qin, Z.N. Chen, J. Photochem. Photobiol., A 194 (2008) 49–58.
[16] B.D. Wang, Z.Y. Yang, J. Fluorescence 18 (2008) 547–553.
[17] B.D. Wang, Z.Y. Yang, P. Crewdson, D.Q. Wang, J. Inorg. Biochem. 101 (2007) 1492–1504.
[18] S. Satyanarayana, J.C. Dabrowiak, J.B. Chaires, Biochemistry 31 (1992) 9319–9324.
[19] C.V. Kumar, E.H. Asuncion, J. Am. Chem. Soc. 115 (1993) 8547–8553.
[20] J. Olmsted III, J. Phys. Chem. 83 (1979) 2581–2584.
[21] J.X. Yu, F.M. Liu, W.J. Lu, Y.P. Li, X.M. Zao, Y.T. Liu, C. Liu, Chin. J. Org. Chem. 20 (2000) 72–80.
[22] J.L. Boyer, J.E. Krum, M.C. Myers, A.N. Fazal, C.T. Wigal, J. Org. Chem. 65 (2000) 4712–4714.
[23] W.J. Geary, Coord. Chem. Rev. 7 (1971) 81–122.
[24] W.T. Carnall, S. Siegel, J.R. Ferraro, B. Tani, E. Gebert, Inorg. Chem. 12 (1973) 560–564.
[25] B. Lippert, C.J.L. Lock, B. Rosenberg, M. Zvagulis, Inorg. Chem. 16 (1977) 1525.
[26] Y. Hirashima, K. Kanetsuki, I. Yonezu, K. Kamakura, J. Shiokawa, Bull. Chem. Soc. Jpn. 56 (1983) 738–743.
[27] C.L. Dollberg, C. Turro, Inorg. Chem. 40 (2001) 2484–2485.
[28] J.M. Kelly, A.B. Tossi, D.J. McConnell, C. OhUigin, Nucleic Acids Res. 13 (1985) 6017–6034.
[29] A.M. Pyle, J.P. Rehmann, R. Meshoyrer, C.V. Kumar, N.J. Turro, J.K. Barton, J. Am. Chem. Soc. 111 (1989) 3051–3058.
[30] G.M. Howe, K.C. Wu, W.R. Bauer, Biochemistry 19 (1976) 339–347.
[31] D.D. Qin, Z.Y. Yang, B.D. Wang, Spectrochim. Acta, Part A 68A (2007) 912–917.
[32] Z.Y. Yang, B.D. Wang, Y.H. Li, J. Organomet. Chem. 691 (2006).
[33] H. Xu, K.C. Zheng, L.J. Lin, H. Li, Y. Gao, L.N. Ji, J. Inorg. Biochem. 98 (2004) 87–97.
[34] V.I. Ivanov, L.E. Minchenkova, A.K. Shchelkina, A.I. Poletaev, Biopolymers 12 (1973) 89–110.
[35] P. Lincoln, E. Tuite, B. Norden, J. Am. Chem. Soc. 119 (1997) 1454–1455.
[36] B. Norden, F. Tjerneld, Biopolymers 21 (1982) 1713–1734.
[37] P. Uma Maheswari, M. Palaniandavar, J. Inorg. Biochem. 98 (2004) 219–230.
[38] C.V. Kumar, J.K. Barton, N.J. Turro, J. Am. Chem. Soc. 107 (1985) 5518–5523.
[39] S. Satyanarayana, J.C. Dabrowiak, J.B. Chaires, Biochemistry 32 (1993) 2573–2584.
[40] M. Eriksson, M. Leijon, C. Hiort, B. Norden, A. Graslund, Biochemistry 33 (1994) 5031–5040.